

Characterization of the Peptidoglycan of Vancomycin-Susceptible *Enterococcus faecium*[†]

Gary J. Patti, Sung Joon Kim, and Jacob Schaefer*

Department of Chemistry, Washington University, One Brookings Drive, St. Louis, Missouri 63130

Received May 3, 2008; Revised Manuscript Received June 9, 2008

ABSTRACT: Vancomycin and other antibacterial glycopeptide analogues target the cell wall and affect the enzymatic processes involved with cell-wall biosynthesis. Understanding the structure and organization of the peptidoglycan is the first step in establishing the mode of action of these glycopeptides. We have used solid-state NMR to determine the relative concentrations of stem-links (64%), bridge-links (61%), and cross-links (49%) in the cell walls of vancomycin-susceptible *Enterococcus faecium* (ATTC 49624). Furthermore, we have determined that *in vivo* only 7% of the peptidoglycan stems terminate in D-Ala-D-Ala, the well-known vancomycin-binding site. Presumably, D-Ala-D-Ala is cleaved from uncross-linked stems in mature peptidoglycan by an active carboxypeptidase. We believe that most of the few pentapeptide stems ending in D-Ala-D-Ala occur in the template and nascent peptidoglycan strands that are crucial for cell-wall biosynthesis.

Enterococci have emerged as life-threatening nosocomial pathogens. These organisms, particularly *E. faecium*, are becoming increasingly resistant to the so-called drug of last resort, vancomycin. This presents a significant clinical challenge because *E. faecium* has an intrinsic resistance to other antibiotics, possibly an adaptation to extended exposure to antimicrobials in the gastrointestinal tract.

Vancomycin targets the bacterial cell wall, inhibiting peptidoglycan (PG)¹ biosynthesis in susceptible organisms by forming complexes with PG precursors (1). To overcome vancomycin, bacteria must alter their structural chemistry, a difficult modification. It was of major concern in 1986 when the first cases of vancomycin-resistant *E. faecium* were reported in Europe (2). One year later a vancomycin-resistant enterococcus (VRE) clinical isolate was detected in the United States (3). Enterococcal infections resistant to vancomycin have increased dramatically around the world since. Over 90% of *E. faecium* isolates are resistant to vancomycin in some hospitals (4). The need to find therapeutic options for treatment of these infections is imperative. Understanding the tertiary structure and organization of the cell wall is critical to characterizing the mechanism of action of vancomycin and its analogues at the molecular level, insights necessary for the successful development of new drugs.

Vancomycin resistance in enterococci is generally associated with a modification of the PG stem termini from D-Ala-D-Ala to D-Ala-D-Lac (5). The substitution exchanges a

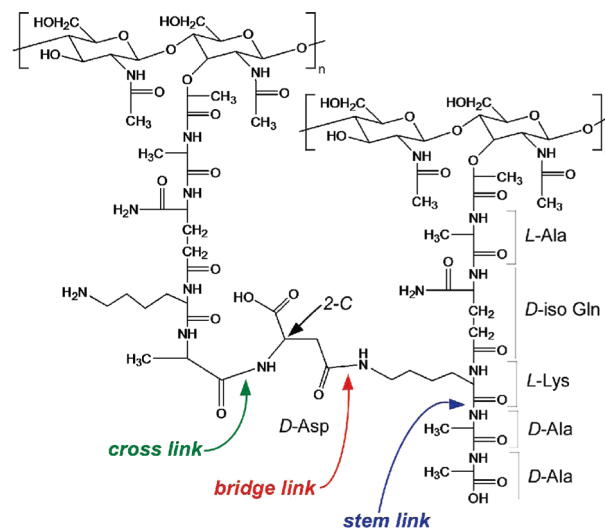


FIGURE 1: Chemical structure of the peptidoglycan of *E. faecium*. The repeat unit on the right is stem-linked and bridge-linked, but not cross-linked. The repeat unit on the left is stem-linked and cross-linked, but not bridge-linked. D-Asp may be amidated.

nitrogen atom in a D-Ala-D-Ala amide bond for an oxygen atom in a D-Ala-D-Lac ester bond. This eliminates a hydrogen bond between the nitrogen of the terminal D-Ala and the oxygen of vancomycin, and substitutes an oxygen–oxygen repulsive interaction. The result is an *in vitro* binding affinity that is reduced 1000-fold for the vancomycin-stem complex (6).

In this article we provide an accurate analysis of the PG composition of an *E. faecium* vancomycin-susceptible organism. The percentages of stem-links, bridge-links, and cross-links (Figure 1) were determined on average to be 64, 61, and 49%, respectively, based on solid-state NMR measurements of both cell-wall isolates and whole-cell preparations. In addition, the number of PG stems terminating in D-Ala-D-Ala was determined *in vivo* to be just 7%, surprisingly

[†] This article is based on work supported by the National Institutes of Health under grant number EB002058.

* To whom correspondence should be addressed. Tel: 314-935-6844. Fax: 314-935-4481. E-mail: jschaefer@wustl.edu.

¹ Abbreviations: CPMAS, cross-polarization magic-angle spinning; ESM, enterococcal standard media; Lipid II, *N*-acetylglucosamine-*N*-acetyl-muramyl-pentapeptide-pyrophosphoryl-undecaprenol; MIC, minimum inhibitory concentration; PG, peptidoglycan; REDOR, rotational-echo double resonance; TA, teichoic acid; VRE, vancomycin-resistant enterococci; VSE, vancomycin-sensitive enterococci.

low considering that this organism is susceptible to vancomycin. We speculate that D-Ala-D-Ala is cleaved from uncross-linked stems by an active carboxypeptidase in mature PG, and that the few remaining pentapeptide stems occur only in template and nascent PG stems that are crucial for cell-wall biosynthesis (7, 8).

EXPERIMENTAL PROCEDURES

Preparation of *E. faecium* and *S. aureus* Samples. Starting cultures of *E. faecium* (ATTC 49624) were prepared by inoculating brain heart infusion media with a single colony. Cultures were incubated overnight at 37 °C, but not aerated. NMR samples were prepared by inoculating sterile enterococcal standard media (ESM) with the overnight starter cultures (1% final volume).

ESM was prepared to contain the following on a per liter basis: 10 g of D-glucose, 20 mg of biotin, 5 mg each of uracil, guanine, cytosine, adenine, and xanthine, 1 mg of inositol, 500 mg of citric acid, 4.1 g of KH_2PO_4 , 4.2 g of $\text{K}_2\text{HPO}_4 \cdot 3\text{H}_2\text{O}$, 1 g of ammonium sulfate, 10 mg of sodium chloride, 100 mg of each of the 20 common amino acids, 100 mg of thiamine hydrochloride, 1 mg each of copper chloride, calcium chloride, copper sulfate, zinc sulfate, and of EDTA, 10 mg each of iron sulfate and of manganese sulfate, 30 mg of magnesium sulfate, 100 μg each of boric acid and of $\text{NiAc}_2 \cdot 4(\text{H}_2\text{O})$, 200 μg each of $\text{Na}_2\text{MoO}_4 \cdot 2(\text{H}_2\text{O})$ and of folic acid, 50 μg of p-aminobenzoic acid, 20 mg of pyridoxine hydrochloride, 2 mg each of pantoic acid, niacin, and of riboflavin, and 10 μg of cyanocobalamin. The pH of ESM was adjusted to 7.0 prior to sterile filtration.

Natural abundance amino acids in ESM were replaced by stable ^{13}C and ^{15}N isotope-enriched amino acids to incorporate specific labels into the samples. When samples were enriched with aspartic acid, asparagine was omitted from the media. All samples enriched with D-[1- ^{13}C]alanine or D-[^{15}N]alanine were treated with 5 $\mu\text{g}/\text{mL}$ of alaphosphin every 1.5 h of growth to prevent conversion of the label to L-alanine.

Cells were harvested at log phase, at a 660 nm absorbance of approximately 1.0, by centrifugation at 10,000 g for 25 min at 4 °C. Pellets were rinsed with 40 mM triethanolamine hydrochloride (pH 7.0) three times, centrifuging after each rinse. Cells were then resuspended in a minimum amount of triethanolamine hydrochloride, frozen, and lyophilized. *Staphylococcus aureus* (ATTC 6538P) samples were prepared similarly, but grown in SASM (*Staphylococcus aureus* standard media) with aeration as detailed previously (9). Cell-wall isolates were prepared from lyophilized whole cells as described before (9).

Solid-State NMR Measurements. Experiments were performed using a four-frequency transmission-line probe (10) with a 14-mm long, 9-mm inside-diameter analytical coil, and a Chemagnetics/Varian magic-angle spinning ceramic stator. Lyophilized samples were spun in Chemagnetics/Varian 7.5-mm outside-diameter zirconia rotors at 5.0 kHz. The speed was under active control and maintained to within ± 2 Hz. Experiments were done at room temperature using a Chemagnetics CMX-300 spectrometer operating at 75.453 MHz for carbon. Radio frequency pulses were produced by 1-kW Kalmus, ENI, and American Microwave Technology power amplifiers, each under active control (11); π pulse lengths were 10 μs for ^{13}C and ^{15}N . Proton-carbon and

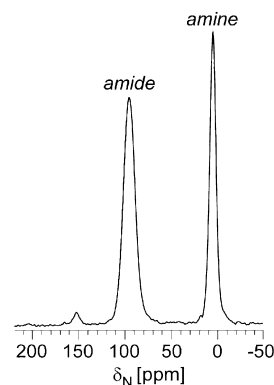


FIGURE 2: ^{15}N CPMAS echo-spectrum of cell-wall isolates enriched with L-[6- ^{15}N]lysine. The amide peak at 95 ppm occurs when lysine forms a bridge-link, and the amine peak at 5 ppm is from lysine that is not bridge-linked. The ratio of the peaks shows that 61% of stems are bridge-linked. The peak at 151 ppm may be the result of a cyclic imide involving the side chain of lysine.

proton-nitrogen cross-polarization transfers were at 50 kHz for 2 msec, unless a T_{IS} experiment was being performed to examine cross-polarization dynamics. Proton dipolar decoupling was 105 kHz during data acquisition. Whole cell and cell-wall samples were typically from 1 and 4 L preparations, respectively. Samples had masses on the order of 300 mg. Each REDOR spectrum typically resulted from 20,000 acquisition scans.

REDOR Experiments. REDOR experiments are performed in two parts: once with dephasing pulses (S) and once without (S_0) (12). In the first part of the experiment, the dephasing pulses are off and magic angle spinning spatially averages chemical-shift and dipolar anisotropic interactions to produce a signal of full intensity. In the second part of the experiment, π -pulses are applied on the dephasing channel to reintroduce the dipolar coupling between spins and produce a reduction in echo-signal intensity. The difference in signal intensity ($\Delta S = S_0 - S$) is directly related to the internuclear distance between the observed and dephasing spins. For one-bond ^{13}C – ^{15}N dipolar coupling, total dephasing is observed after 8 T_r with 5-kHz magic-angle spinning ($T_r = 0.2$ ms).

Uncertainties in REDOR dephasing measurements were estimated using integrals of ΔS (8). For all of the spectra shown, the error was less than 3%, typical for short evolution-time REDOR experiments over one-bond distances.

RESULTS

Bridge-Links in Cell-Wall Isolates. An ^{15}N cross-polarization magic-angle spinning (CPMAS) echo spectrum of *E. faecium* cell-wall isolates enriched with L-[6- ^{15}N]lysine (Figure 2) provides the percentage of PG bridge-links. The side chain of lysine forms an amide (95 ppm) when it is bridge-linked and is an amine (5 ppm) when it is not bridge-linked. Metabolic scrambling of lysine is minimal, so a comparison of the amide to amine peak provides the percentage of bridge-links directly. To account for rotating-frame dynamics in cross-polarization and relaxation between amides and amines, the integral of each peak was obtained as a function of cross-polarization contact time (13). Extrapolating to zero contact time provides an amide to amine ratio of 61 to 39, indicating that 61% of all PG stems are bridge-linked.

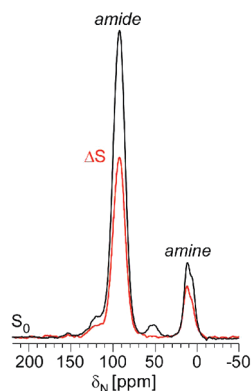


FIGURE 3: $^{15}\text{N}\{^{13}\text{C}\}$ REDOR spectra after $8\text{-}T_r$ evolution time of *E. faecium* cell-wall isolates enriched with D,L- ^{15}N , 2- ^{13}C aspartic acid. Bridges that are cross-linked form amides, and those that do not remain amines. Nitrogen label that was scrambled by aminotransferase does not dephase after $8\text{-}T_r$. The full-echo spectrum is in black and the REDOR difference in red. Eighty-three percent of bridges are cross-linked, as determined by the relative integrated intensities of the amide and amine peaks of the REDOR difference spectrum.

Cross-Links in Cell-Wall Isolates. An ^{15}N CPMAS echo experiment on ^{15}N aspartic-acid-enriched cell walls does not directly provide an accurate measure of cross-linking because the nitrogen of aspartic acid is readily scrambled by aminotransferase activity. To account for scrambling, cell-wall isolates double labeled with D,L- ^{15}N , 2- ^{13}C aspartic acid were prepared (see Figure 1). Only ^{15}N labels that dephase by a directly bonded ^{13}C are considered in determining the ratio of aspartic acid amides to amines. A ratio of 83 amides to 17 amines is obtained from ΔS after $8\text{-}T_r$ (Figure 3, red) after rotating-frame dynamics are accounted for. However, this ratio only describes PG stems with aspartic acid bridges. To determine the percentage of total PG stems that are cross-linked from the aspartic-acid labeling, the percentage of stems with bridge-links (61%) is multiplied by the fraction of cross-linked bridges (0.83). Thus, the percentage of cross-linking is $61\% \times 0.83 = 51\%$.

Specific Labeling of D-Alanine. In *E. faecium*, alanine racemase catalyzes the isomerization of D- and L-alanine (14). To specifically label D-alanine, the enzyme must be inhibited with alaphosphin (15). Because *E. faecium* metabolizes alaphosphin, the alanine-racemase inhibitor was added every 1.5 h of growth at $5\text{ }\mu\text{g/mL}$. Inhibition under these conditions was verified with rescue-growth experiments. When *E. faecium* was provided only L-alanine in the presence of alaphosphin, growth was inhibited (Figure 4) because D-alanine is required for cell-wall biosynthesis.

Stem-Links in Cell-Wall Isolates. Cell-wall isolates were prepared from whole cells enriched with L-[1- ^{13}C]lysine and D-[^{15}N]alanine, grown in the presence of alaphosphin. When lysine is stem-linked (see Figure 1), the carbonyl carbon forms a peptide bond with a chemical shift of 174 ppm. Lysine that is not stem-linked has a carboxyl terminus with a chemical shift of 178 ppm (15). The percentage of stem-links can be obtained by deconvoluting a ^{13}C CPMAS echo spectrum (Figure 5). The line shape of the 174-ppm carbonyl peptide peak used in the deconvolution was provided experimentally by ΔS from a $^{13}\text{C}\{^{15}\text{N}\}$ REDOR experiment. When ΔS is scaled so that no residual intensity remains at 174 ppm in the CPMAS echo spectrum, the residual, which represents carboxyl termini, has an identical line shape to

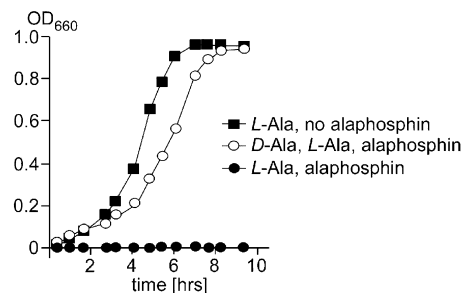


FIGURE 4: One-liter growths of *E. faecium* in the presence and absence of alaphosphin, an alanine racemase inhibitor. Alaphosphin was added every 1.5 h of growth at $5\text{ }\mu\text{g/mL}$. *E. faecium* cannot survive in the presence of alaphosphin without exogenous D-Ala.

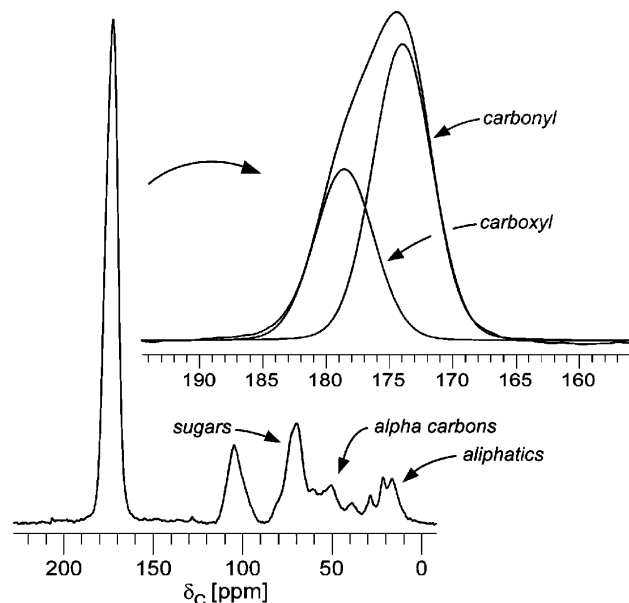


FIGURE 5: ^{13}C CPMAS echo spectrum of cell-wall isolates enriched with L-[1- ^{13}C]lysine. The carbonyl-carbon peak is deconvoluted into two components, a 178-ppm carboxyl peak and a 174-ppm carbonyl-carbon peak (inset). The line shape of the 174-ppm peak was determined by REDOR (see Figure 6, top inset). The ratio of the two peak intensities shows that 64% of L-lysine is stem-linked.

that of ΔS (15). We determine that 64% of PG stems have L-Lys-D-Ala linkages from the ratio of the 174 ppm to 178 ppm peaks in the deconvolution. The same CPMAS deconvolution was observed for a sample prepared without alaphosphin, verifying that the inhibitor did not affect the stem-link ratio.

The $\Delta S/S_0$ for the 174-ppm carbonyl peptide peak determines the enrichment of D-[^{15}N]alanine, a factor required to quantify the relative concentration of stem-links for intact whole cells (see below). Because enrichment factors are the same in cell-wall isolates and whole cells, analysis of cell-wall isolates could be used to determine the enrichment thereby avoiding complications from cytoplasmic proteins. The maximum one-bond dephasing at $8\text{-}T_r$ (Figure 6, top left inset), taken with respect to the carbonyl-carbon peak at 174 ppm from deconvolution (Figure 6, bottom left inset) shows directly that the enrichment of D-[^{15}N]alanine is 64%.

Aspartic Acid Enrichment. Cell walls isolated from whole cells, grown in the presence of alaphosphin and enriched with L-[6- ^{15}N]lysine and D,L-[4- ^{13}C]aspartic acid, were analyzed using $^{15}\text{N}\{^{13}\text{C}\}$ REDOR. L-[6- ^{15}N]lysine bridge-linked to aspartic acid forms an amide, chemically shifted

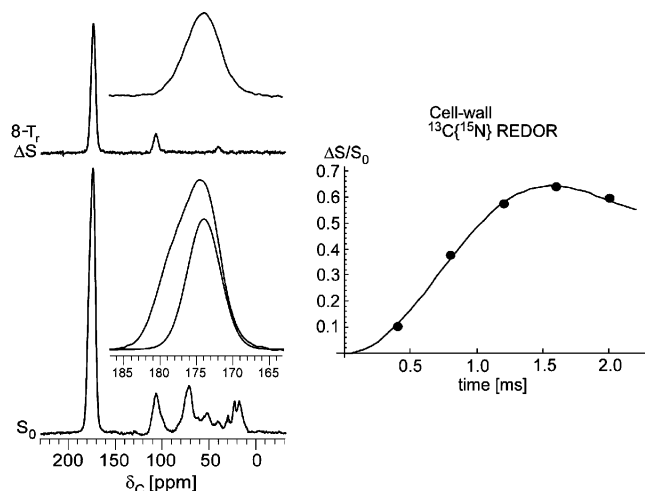


FIGURE 6: (Left) $^{13}\text{C}\{^{15}\text{N}\}$ REDOR spectra after $8\text{-}T_r$ evolution time for cell walls isolated from whole cells labeled with L-[1- ^{13}C]lysine and D-[^{15}N]alanine, grown in the presence of alaphosphin. The full-echo spectrum (S_0) is shown at the bottom of the figure and the REDOR difference (ΔS) at the top. The carbonyl region of the full-echo spectrum is deconvoluted in the lower inset, showing the fraction of stem-linked lysine at 174 ppm. The REDOR difference of the top inset (same expanded scale) provided the line shape for the 174-ppm component of the deconvolution. (Right) $^{13}\text{C}\{^{15}\text{N}\}$ REDOR dephasing ($\Delta S/S_0$) of the 174-ppm component of the carbonyl-carbon peak as a function of dipolar evolution time. The maximum one-bond dephasing shows the isotopic enrichment of D-[^{15}N]alanine is 64%. The enrichment of D-[^{15}N]alanine is independent of stem-linking; the fact that 64% of the PG in cell-wall isolates is stem-linked is a coincidence.

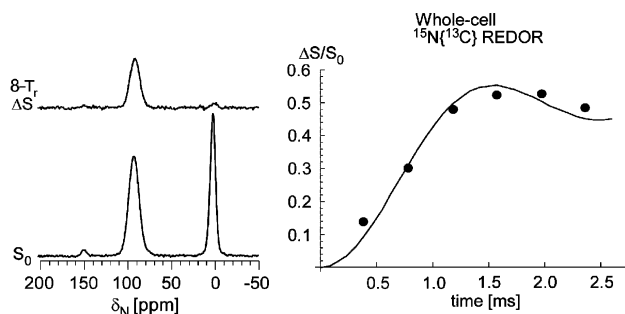


FIGURE 7: (Left) $^{15}\text{N}\{^{13}\text{C}\}$ REDOR spectra after $8\text{-}T_r$ evolution time for cell-wall isolates enriched with L-[6- ^{15}N]lysine and D,L-[4- ^{13}C]aspartic acid, grown in the presence of alaphosphin. (Right) $^{15}\text{N}\{^{13}\text{C}\}$ REDOR dephasing ($\Delta S/S_0$) of the 95-ppm peak as a function of dipolar evolution time. The maximum one-bond dephasing shows that the isotopic enrichment of D,L-[4- ^{13}C]aspartic acid is 55%.

to 95 ppm (Figure 7, left). The maximum one-bond dephasing of amidated L-[6- ^{15}N]lysine shows that the enrichment of 4- ^{13}C aspartic acid is 55% (Figure 7, right). The enrichment of 2- ^{13}C in aspartic acid is the same as that of 4- ^{13}C . Cell walls double labeled by D,L-[2- ^{13}C , ^{15}N] aspartic acid, analyzed with $^{13}\text{C}\{^{15}\text{N}\}$ REDOR, showed that the 2- ^{13}C peak at 50 ppm dephases completely to natural-abundance ^{13}C levels (Figure 8). Thus, the ^{15}N aspartic acid enrichment is the same as that of 2- ^{13}C , 55%.

Stem-Links in Whole Cells. $^{13}\text{C}\{^{15}\text{N}\}$ REDOR was used to determine stem-linking in whole cells enriched with L-[1- ^{13}C]lysine and D-[^{15}N]alanine, grown in the presence of alaphosphin. Only the peak centered around 175 ppm was considered (Figure 9), as the spinning side bands have the same line shape and dephasing ratios. The center band has contributions from proteins and PG stems. PG tripeptide

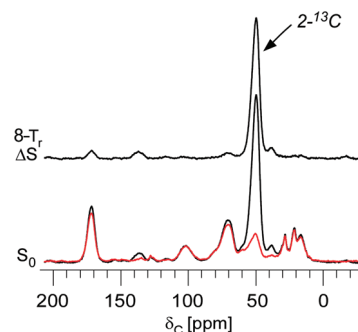


FIGURE 8: $^{13}\text{C}\{^{15}\text{N}\}$ REDOR spectra for cell-wall isolates enriched with D,L-[2- ^{13}C , ^{15}N]aspartic acid. The alpha-carbon peak near 50 ppm has approximately the same intensity as that of a natural-abundance aliphatic-carbon peak (see Figure 5). The dephased spectrum, S (bottom, red), is superimposed on S_0 (bottom, black) to illustrate that dephasing reaches natural-abundance levels at $8\text{-}T_r$. The total dephasing verifies that the enrichment of ^{15}N in aspartic acid is equal to that of 4- ^{13}C in aspartic acid, which is the same as that of 2- ^{13}C (55%, see Figure 7).

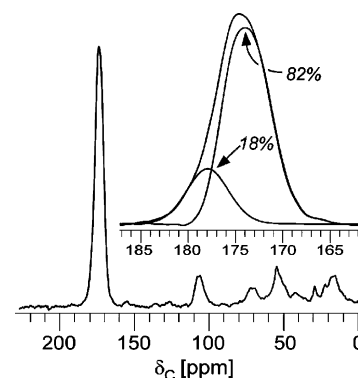


FIGURE 9: ^{13}C CPMAS echo spectrum of whole cells enriched with L-[1- ^{13}C]lysine. The carboxyl lysine peak at 178 ppm is unique to the cell wall, and its intensity can be determined by deconvolution using the line shape obtained from cell-wall isolates (inset). The lysine carboxyl termini represent 18% of the peak intensity, with stem-linked PG and cytoplasmic proteins accounting for the remaining 82%.

stems terminate in lysine, and these lysine carboxyl carbons at 178 ppm are unique to the cell wall. The whole-cell L-[1- ^{13}C]lysine CPMAS spectrum is deconvoluted, using the same line shape from cell-wall isolates, so that no residual intensity at 178 ppm remains (Figure 9, inset). The 178-ppm peak is 18% of the total. The remaining 82% at 174 ppm is due to proteins and stem-linked PG.

Results from $^{13}\text{C}\{^{15}\text{N}\}$ REDOR on whole cells (Figure 10) can be used to deconvolute experimentally contributions of stem-linked PG from those of the proteins at 174 ppm. The 19% dephasing maximum after $8\text{-}T_r$ for the total carbonyl-carbon peak, scaled by the 174-ppm peak intensity and by the enrichment of D-[^{15}N]alanine ($1/0.64 = 1.56$), provides the fraction of stem-linked PG in the 174-ppm peak. That is, $(19/82) \times 1.56 = 0.36$. Because 36% of the 174-ppm peak is 30% of the total carbonyl-carbon peak, the ratio of 30:18 is the ratio of stem-linked PG to tripeptides in whole cells, a normalized ratio of 63:37.

Cross-Links in Whole Cells. Solid-state NMR provides a method to measure cross-linking in whole cells. The analysis exploits the fact that D-alanine is exclusively incorporated into the cell wall in PG stems and alanyl ester side chains of teichoic and lipoteichoic acids (15). Whole-cell *E. faecium* samples were prepared enriched with D,L-[^{15}N]aspartic acid

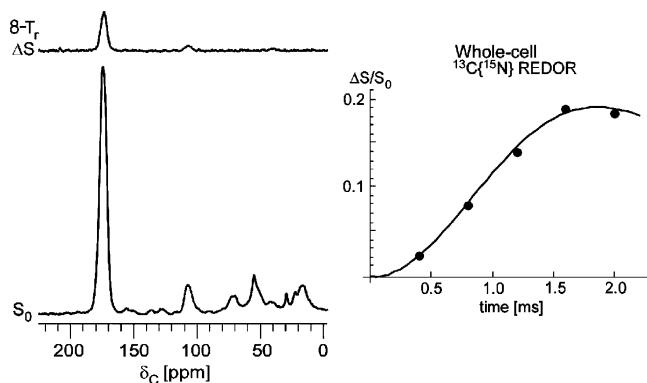


FIGURE 10: (Left) $^{13}\text{C}\{^{15}\text{N}\}$ REDOR spectra after $8\text{-}T_r$ evolution time for whole cells enriched with L-[$1\text{-}^{13}\text{C}$]lysine and D-[^{15}N]alanine, grown in the presence of alaphosphin. Only stem-linked lysyl carbonyl carbons in PG dephase after $8\text{-}T_r$. (Right) $^{13}\text{C}\{^{15}\text{N}\}$ REDOR dephasing ($\Delta S/S_0$) of the total carbonyl-carbon peak as a function of dipolar evolution time. The maximum one-bond dephasing is 19%.

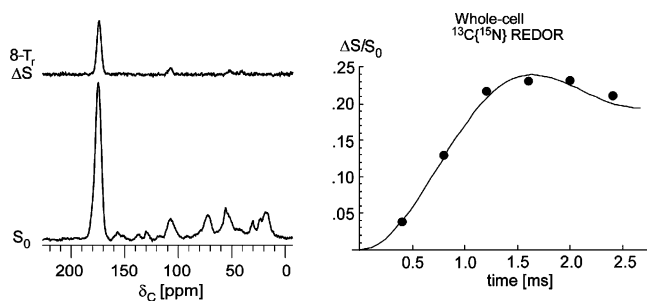


FIGURE 11: (Left) $^{13}\text{C}\{^{15}\text{N}\}$ REDOR spectra after $8\text{-}T_r$ evolution time for whole cells enriched with D-[$1\text{-}^{13}\text{C}$]alanine and D,L-[^{15}N]aspartic acid, grown in the presence of alaphosphin. The REDOR difference spectrum, ΔS , represents only D-Ala cross-linked to D-Asp. (Right) $^{13}\text{C}\{^{15}\text{N}\}$ REDOR dephasing ($\Delta S/S_0$) of the 175-ppm peak as a function of dipolar evolution time. The maximum one-bond dephasing is 24%.

and D-[$1\text{-}^{13}\text{C}$]alanine from growths in the presence of alaphosphin. In a $^{13}\text{C}\{^{15}\text{N}\}$ REDOR experiment, only cross-linked D-[$1\text{-}^{13}\text{C}$]alanine labels dephase after $8\text{-}T_r$ (Figure 11, left). The REDOR ΔS at 175 ppm is specific to D-Ala peptide carbonyl carbons in cross-linked stems. There are four other D-Ala carbonyl contributions to the total carbonyl-carbon peak that do not dephase (15): (i) the peptide carbonyl of D-Ala in D-Ala-D-Ala stems whose signal is at 175 ppm; (ii) the D-Ala terminal carboxyl of these stems at 178 ppm; (iii) the D-Ala terminal carboxyl on uncross-linked stems with only one D-Ala; and (iv) various teichoic D-Ala esters at 172 ppm (Figure 12).

The one-bond maximum dephasing, 24% by integration (Figure 11, right), represents the amount of D-alanine forming bonds with enriched D-aspartic acid. However, because D-aspartic acid is only 55% enriched and the carbonyl natural-abundance contribution was determined to be 19% in a separate experiment, we multiply ΔS by 1.82 ($1/0.55$) to account for D-aspartic acid enrichment and divide by 0.81 to remove the 19% carbonyl natural-abundance contribution: $(0.24 \times 1.82)/0.81 = 0.54$. The scaled ΔS represents the intensity of those D-Ala bonded to D-Asp and is used to deconvolute S_0 experimentally.

When the scaled ΔS is removed from S_0 , the remaining S_0 intensity at 175 ppm is small. Thus there can be relatively few stems containing D-Ala-D-Ala, which have a 175-ppm

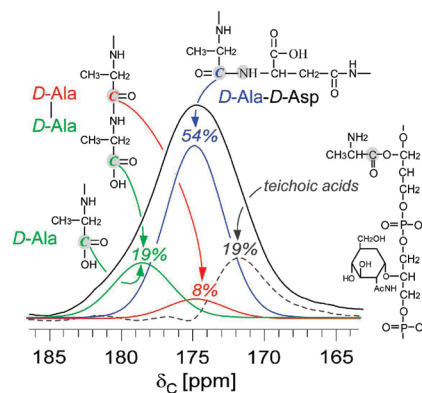


FIGURE 12: Complete experimental deconvolution of the carbonyl-carbon ^{13}C spectrum of whole cells enriched with D-[$1\text{-}^{13}\text{C}$]alanine and D,L-[^{15}N]aspartic acid grown in the presence of alaphosphin. The percentages show the distribution of D-Ala in *E. faecium* cell walls (see text).

Table 1: Distribution of PG Stems in the Cell Wall of *E. faecium*

stem	1 [%]	2 [%]	3 [%]
D-Ala-D-Asp ^{a-c}	54	74	47
D-Ala-D-Ala	8	11	7
D-Ala	11	15	9

^a Column 1: relative concentrations of D-Ala stems from CPMAS deconvolution (Figure 12). On the basis of the results for three different growths, relative concentrations are 54 ± 1 , 8 ± 1 , and 11 ± 1 .

^b Column 2: percentages with respect to stem-linked PG (column 1/0.73). ^c Column 3: percentages with respect to total PG (column 2 \times 0.63).

carbonyl carbon. The ratio is quantified by using the line shape of ΔS as a model to fit both the 178-ppm carboxyl carbon of D-Ala termini and the 175-ppm carbonyl peptide of D-Ala on D-Ala-D-Ala stems. ΔS is centered at 178 ppm and scaled so that no residual intensity at the 178-ppm carboxyl-carbon region remains after subtraction. Similarly, ΔS is scaled to fit D-Ala carbonyl carbons remaining at 175 ppm so that no residual intensity remains after subtraction. The resultant of the full deconvolution represents D-Ala teichoic esters. Each component taken with respect to the total peak (natural abundance removed) provides the distribution of D-Ala label: 54% of the total peak is from D-Ala in D-Ala-D-Asp cross-linked stems, 19% is from D-Ala termini, 8% is from D-Ala peptides in D-Ala-D-Ala stems, and 19% is from D-Ala esters in teichoic acids (Figure 12).

A small number of uncross-linked stems terminate in a single D-alanine. Because each D-Ala-D-Ala stem must contain a peptide carbonyl and a terminal carboxyl D-Ala, uncross-linked stems containing a single D-Ala can be obtained by subtracting the D-Ala-D-Ala 175 ppm carbonyl peak from the 178-ppm peak. That is, 19 minus 8 equals 11%.

To calculate total cross-linking, the data must be normalized to all PG stems (Table 1). First the percentages are taken with respect to the total number of D-Ala containing stems. This excludes teichoic acids and counts D-Ala-D-Ala stems only once. The relative number of D-Ala containing stems is 54, from D-Ala-D-Asp, plus 19, because all other stems terminate with a carboxyl D-Ala (Figure 12), for a total of 73. When the PG stem percentages are normalized to 0.73, the distribution of D-Ala containing stems is obtained: $54/0.73 = 74\%$ D-Ala-D-Asp; $8/0.73 = 11\%$ D-Ala-D-Ala; and $11/0.73 = 15\%$ stems with a single D-Ala. This distribution,

Table 2: *E. faecium* and *S. aureus* Cell-Wall Comparison

organism	bridge-links (cell walls) [%]	stem-links (cell walls) [%]	stem-links (whole cells) [%]	cross-links (cell walls) [%]	cross-links (whole cells) [%]	TA:PG (D-Ala)
<i>E. faecium</i> ^a	61	64	63	51	47	0.17:1
<i>S. aureus</i> ^a	85	100	100	67	54	1:1

^a The estimated error in REDOR-determined bridge-links, stem-links, and cross-links is $\pm 2\%$.

however, only accounts for PG with stem-links which is determined by solid-state NMR to be 63% overall in whole cells (Table 2). The values are renormalized to 63% to get ratios with respect to total PG composition. Thus, in whole cells, 47% of stems are cross-linked (63×0.74), 7% end in D-Ala-D-Ala (63×0.11), 9% terminate in a single D-Ala (63×0.15), and the remaining 37% are tripeptides (Table 1).

Cross-Linking in *Staphylococcus aureus*. *S. aureus* cell walls enriched with [¹⁵N]glycine were prepared exactly as described for *E. faecium* for comparative purposes. ¹⁵N CPMAS spectra were consistent with those shown previously (bottom left of Figure 7 in ref 9). The *S. aureus* PG amino acid composition is similar to *E. faecium*, but the bridge has five glycine residues. The fifth glycine forms an amide when cross-linked, but is otherwise an amine. The ¹⁵N CPMAS experiment measures the extent of cross-linking, but is complicated by the other four glycine residues in the bridge. After cross-polarization effects are accounted for, the ratio of amides to amines is 23:1. Each amine represents an uncross-linked bridge, with four glycine residues forming amides. Thus, for the 1 amine, 4 amides can be subtracted in the ratio. This makes a new ratio of 19:1. Each cross-linked glycine also has four other glycine amides in the bridge. So 19 is divided by five to obtain the ratio of cross-linked bridges to uncross-linked bridges, which is 3.8:1. Thus, 79% of *S. aureus* bridges are cross-linked. However, only 85% of stems have bridges (left of Figure 7 in ref 16). The total cross-linking in *S. aureus* is therefore $85\% \times 0.79 = 67\%$, compared to 51% in *E. faecium* (Table 2). Unlike the situation in *E. faecium*, PG without stem-links has not been reported in *S. aureus* (17).

DISCUSSION

D,D-Carboxypeptidase in VSE. The 9% of uncross-linked PG stems terminating in a single D-Ala (Table 1) suggests D,D-carboxypeptidase activity that is independent of transpeptidation. This is an unexpected finding for a VSE organism because D,D-carboxypeptidase activity is thought to be associated with vancomycin resistance, a mechanism to eliminate potential glycopeptide-binding sites. It seems implausible that a substantial increase in D,D-carboxypeptidase activity in resistant organisms (18) would be required to cleave just the 7% of D-Ala-D-Ala terminated stems that remain. Our data are therefore inconsistent with the hypothesis (18, 19) that increasing levels of vancomycin resistance are directly related to higher levels of D,D-carboxypeptidase activity.

D,D-carboxypeptidase activity has been suggested to be localized to the membrane and to the cytoplasm of *E. faecium* (5). Based on the results presented here, it is not possible to say where the uncross-linked tetrapeptides are. Future solid-state NMR experiments on VSE whole cells harvested midlog phase, after one hour of vancomycin exposure, might

be insightful in this regard. If PG precursors accumulate in the cytoplasm where the D,D-carboxypeptidase is active, a proportional increase in uncross-linked tetrapeptide stems would be observed.

D-Alanylation of Teichoic Acids. A dramatic difference between *E. faecium* and *S. aureus* is the concentration of D-alanine in teichoic acids (Table 2). The D-[1-¹³C]alanine CPMAS deconvolution for *E. faecium* whole cells (Figure 12) shows that 19% of D-Ala is in teichoic acids. This amounts to approximately 0.17 D-Ala in teichoic acids for every 1 PG stem, when the tripeptides are taken into account. In *S. aureus* a similar analysis shows approximately 1 D-Ala in teichoic acids for every 1 PG stem (15). Comparable results were obtained from *S. aureus* grown in ESM. The contrast between the organisms may reflect differences in PG processing as the positively charged D-alanine ester substituents are thought to decrease the binding capacity of the teichoic acids for autolysins by charge compensation (20). The difference in charge distribution may also affect the binding capacity of glycopeptides (21). It has been shown that almost twice the amount of D-Ala is attached to lipoteichoic acids in *E. faecium* expressing vancomycin resistance (22).

PG Homogeneity in *E. faecium*. The *E. faecium* PG characterizations are similar for cell-wall isolates and whole-cell analyses. In cell-wall isolates, 64% of stems are stem-linked and 51% cross-linked (Table 2). In *E. faecium* whole cells, 63% of the PG stems are stem-linked, and 47% cross-linked. This contrasts with the findings for *S. aureus* where cross-linking determinations differ by 13% between whole cells (15) and cell walls (Table 2).

Digestion studies have shown that portions of the *S. aureus* PG are cross-linked as high as 90% (23). We have suggested previously that the distribution of cross-links in the mature cell walls of *S. aureus* is heterogeneous (15). We believe that cell-wall isolations, and other digestion protocols, select for more extensively cross-linked portions of the PG and therefore overestimate cross-linking. Densely cross-linked regions of enterococcal PG have not been detected in digestion studies (24). This seems consistent with the NMR data reported here in that the average cross-linking determinations of *E. faecium* do not significantly differ in whole cells and isolated cell walls. This comparison indicates that enterococcal PG is more homogeneous than the PG of *S. aureus*.

We speculate that *E. faecium* compensates for a lower degree of overall cross-linking, without regions of high density, by lengthening glycan chains to achieve greater structural integrity. In *S. aureus* the average glycan chain length has been determined to be approximately 6 disaccharides with a broad distribution (25), consistent with PG heterogeneity. Measurements of *E. faecium* glycan chain lengths have not been reported, but we suspect that the *E. faecium* distribution will be narrower with a longer

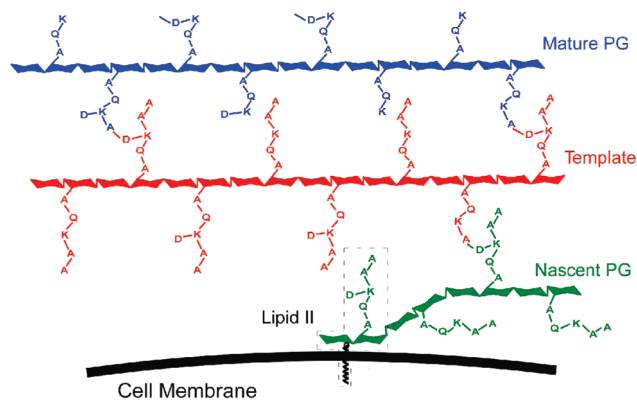


FIGURE 13: Two-dimensional schematic representation of proposed template model of PG assembly in *E. faecium*. Chain extension, occurring from right to left, and cross-linking are synchronized at lipid II, which is bound to the cell-wall membrane. The template strand (red) serves to orient nascent PG (green) so that high levels of cross-linking can be achieved. Tripeptides occur in mature PG (blue), where *L,D*-carboxypeptidase acts on uncross-linked stems. Seven percent of all stems terminating in *D*-Ala-*D*-Ala probably occur in nascent and template PG and are crucial for cell wall assembly. Modification of these few sites and the lipid II sites could prevent some glycopeptides from binding and inhibiting PG biosynthesis.

average length. Glycan chains have been determined in some *Bacillus subtilis* organisms to be as long as 140 disaccharides (26).

Template Model for PG Assembly in *E. faecium*. The *E. faecium* strain investigated in this article is a vancomycin-susceptible organism. Only 7% of PG stems (plus lipid II) have the well-known *D*-Ala-*D*-Ala vancomycin-binding site. We believe that these few pentapeptide PG stems may be crucial to cell-wall biosynthesis. We propose the applicability of a template model of PG assembly in *E. faecium*, previously discussed in connection with *S. aureus* (7, 8). In this model (Figure 13), glycan chain extension and cross-linking occur near the cell membrane with single-strand addition (27, 28). The orientation of the new nascent PG strand is controlled by the stem conformation of the nearest neighbor, the last completed PG chain called the template. The template is only partially cross-linked, having already served as the acceptor to mature PG and acting as the donor to the extending nascent chain. When a cross-link forms, the fourth *D*-Ala serves as a donor forming an amide bond to a bridge and a *D,D*-carboxypeptidase removes the terminal *D*-Ala. Thus, the template strand must have *D*-Ala-*D*-Ala stems in order to form cross-links with nascent PG, a requirement for cell-wall integrity.

We suspect that there is also an active *L,D*-carboxypeptidase in mature PG to account for the high concentration of tripeptide stems (Figure 9). *L,D*-Carboxypeptidase activity has been reported before in other Gram-positive bacteria (29, 30). In mature PG, pentapeptide stems that were not cross-linked are cleaved forming tripeptides. For a cell wall with 15–20 glycan layers, the template and nascent strands represent 5–10% of the total PG. We believe that this fraction corresponds to the 7% of *D*-Ala-*D*-Ala stems observed in our whole-cell NMR experiments. Modification of these sites (and the lipid II sites) would prevent vancomycin from binding (6), although other glycopeptides may still bind and inhibit PG biosynthesis (7).

AUTHORS' CONTRIBUTIONS

G.J.P. designed experiments, prepared samples, acquired data, analyzed and interpreted data, and wrote a first-draft manuscript. S.J.K. contributed to the conception of the experiments. J.S. contributed to the interpretation of the data and revised the manuscript for intellectual content. All authors approved the final version of the manuscript.

REFERENCES

1. Mainardi, J. L., Villet, R., Bugg, T. D., Mayer, C., and Arthur, M. (2008) Evolution of peptidoglycan biosynthesis under the selective pressure of antibiotics in Gram-positive bacteria. *FEMS Microbiol. Rev.* 32, 386–408.
2. Uttley, A. H., Collins, C. H., Naidoo, J., and George, R. C. (1988) Vancomycin-resistant enterococci. *Lancet* 1, 57–58.
3. Johnson, A. P., Uttley, A. H., Woodford, N., and George, R. C. (1990) Resistance to vancomycin and teicoplanin: an emerging clinical problem. *Clin. Microbiol. Rev.* 3, 280–291.
4. Kak, V. a. C., Joseph, W. (2002) *Acquired Antibiotic Resistances in Enterococci*, ASM Press, Washington, DC.
5. Courvalin, P. (2006) Vancomycin resistance in gram-positive cocci. *Clin. Infect. Dis.* 42, S25–S34.
6. Bugg, T. D., Wright, G. D., Dutka-Malen, S., Arthur, M., Courvalin, P., and Walsh, C. T. (1991) Molecular basis for vancomycin resistance in *Enterococcus faecium* BM4147: biosynthesis of a depsipeptide peptidoglycan precursor by vancomycin resistance proteins VanH and VanA. *Biochemistry* 30, 10408–10415.
7. Kim, S. J., Cegelski, L., Stueber, D., Singh, M., Dietrich, E., Tanaka, K. S. E., Parr, T. R., Far, A. R., and Schaefer, J. (2008) Oritavancin exhibits dual mode of action to inhibit cell-wall biosynthesis in *Staphylococcus aureus*. *J. Mol. Biol.* 377, 281–293.
8. Kim, S. J., Matsuoka, S., Patti, G. J., and Schaefer, J. (2008) Vancomycin derivative with damaged *D*-Ala-*D*-Ala binding cleft binds to cross-linked peptidoglycan in the cell wall of *Staphylococcus aureus*. *Biochemistry* 47, 3822–3831.
9. Tong, G., Pan, Y., Dong, H., Pryor, R., Wilson, G. E., and Schaefer, J. (1997) Structure and dynamics of pentaglycyl bridges in the cell walls of *Staphylococcus aureus* by ^{13}C - ^{15}N REDOR NMR. *Biochemistry* 36, 9859–9866.
10. Schaefer, J., McKay, R. A. (1999) Multi-Tuned Single-Coil Transmission-Line Probe for Nuclear Magnetic Resonance Spectrometer, U.S. Patent 5,861,748.
11. Steuber, D., Mehta, A. K., Chen, Z., Wooley, K. L., and Schaefer, J. (2006) Local order in polycarbonate glasses by $^{13}\text{C}\{^{19}\text{F}\}$ rotational-echo double-resonance NMR. *J. Polym. Sci. Part B: Polym. Phys.* 2760–2775.
12. Guillion, T. S. J. (1989) Detection of Weak Heteronuclear dipolar coupling by rotational-echo double-resonance nuclear magnetic resonance. *Adv. Magn. Reson.* 13, 57–83.
13. McDowell, L. M., Schmidt, A., Cohen, E. R., Studelska, D. R., and Schaefer, J. (1996) Structural constraints on the ternary complex of 5-enolpyruvylshikimate-3-phosphate synthase from rotational-echo double-resonance NMR. *J. Mol. Biol.* 256, 160–171.
14. Walsh, C. T. (1989) Enzymes in the *D*-alanine branch of bacterial cell wall peptidoglycan assembly. *J. Biol. Chem.* 264, 2393–2396.
15. Cegelski, L., Steuber, D., Mehta, A. K., Kulp, D. W., Axelsen, P. H., and Schaefer, J. (2006) Conformational and quantitative characterization of oritavancin-peptidoglycan complexes in whole cells of *Staphylococcus aureus* by in vivo ^{13}C and ^{15}N labeling. *J. Mol. Biol.* 357, 1253–1262.
16. Kim, S. J., Cegelski, L., Studelska, D. R., O'Connor, R. D., Mehta, A. K., and Schaefer, J. (2002) Rotational-echo double resonance characterization of vancomycin binding sites in *Staphylococcus aureus*. *Biochemistry* 41, 6967–6977.
17. Giesbrecht, P., Kersten, T., Maidhof, H., and Wecke, J. (1998) *Staphylococcal cell wall: morphogenesis and fatal variations in the presence of penicillin. Microbiol. Mol. Biol. Rev.* 62, 1371–1414.
18. Gutmann, L., Billot-Klein, D., al-Obeid, S., Klare, I., Francoual, S., Collatz, E., and van Heijenoort, J. (1992) Inducible carboxypeptidase activity in vancomycin-resistant enterococci. *Antimicrob. Agents Chemother.* 36, 77–80.

19. al-Obeid, S., Collatz, E., and Gutmann, L. (1990) Mechanism of resistance to vancomycin in *Enterococcus faecium* D366 and *Enterococcus faecalis* A256. *Antimicrob. Agents Chemother.* **34**, 252–256.
20. Wecke, J., Perego, M., and Fischer, W. (1996) D-alanine deprivation of *Bacillus subtilis* teichoic acids is without effect on cell growth and morphology but affects the autolytic activity. *Microb. Drug Resist.* **2**, 123–129.
21. Peschel, A., Vuong, C., Otto, M., and Gotz, F. (2000) The D-alanine residues of *Staphylococcus aureus* teichoic acids alter the susceptibility to vancomycin and the activity of autolytic enzymes. *Antimicrob. Agents Chemother.* **44**, 2845–2847.
22. Gutmann, L., Al-Obeid, S., Billot-Klein, D., Ebnet, E., and Fischer, W. (1996) Penicillin tolerance and modification of lipoteichoic acid associated with expression of vancomycin resistance in VanB-type *Enterococcus faecium* D366. *Antimicrob. Agents Chemother.* **40**, 257–259.
23. Labischinski, H. (1992) Consequences of the interaction of beta-lactam antibiotics with penicillin binding proteins from sensitive and resistant *Staphylococcus aureus* strains. *Med. Microbiol. Immunol.* **181**, 241–265.
24. Billot-Klein, D., Shlaes, D., Bryant, D., Bell, D., van Heijenoort, J., and Gutmann, L. (1996) Peptidoglycan structure of *Enterococcus faecium* expressing vancomycin resistance of the VanB type. *Biochem. J.* **313** (Pt 3), 711–715.
25. Boneca, I. G., Huang, Z. H., Gage, D. A., and Tomasz, A. (2000) Characterization of *Staphylococcus aureus* cell wall glycan strands, evidence for a new beta-N-acetylglucosaminidase activity. *J. Biol. Chem.* **275**, 9910–9918.
26. Archibald, A. R., Hancock, I. C., and Harwood, C. R. (1993) *Cell Wall Structure, Synthesis, and Turnover*, ASM Press, Washington, DC.
27. Gally, D., and Archibald, A. R. (1993) Cell wall assembly in *Staphylococcus aureus*: proposed absence of secondary crosslinking reactions. *J. Gen. Microbiol.* **139**, 1907–1913.
28. Gally, D. L., Hancock, I. C., Harwood, C. R., and Archibald, A. R. (1991) Cell wall assembly in *Bacillus megaterium*: incorporation of new peptidoglycan by a monomer addition process. *J. Bacteriol.* **173**, 2548–2555.
29. Courtin, P., Miranda, G., Guillot, A., Wessner, F., Mezange, C., Domakova, E., Kulakauskas, S., and Chapot-Chartier, M. P. (2006) Peptidoglycan structure analysis of *Lactococcus lactis* reveals the presence of an L,D-carboxypeptidase involved in peptidoglycan maturation. *J. Bacteriol.* **188**, 5293–5298.
30. Hammes, W. P. (1978) The LD-carboxypeptidase activity in *Gaffkya homari*. The target of the action of D-amino acids or glycine on the formation of wall-bound peptidoglycan. *Eur. J. Biochem.* **91**, 501–507.

BI8008032